AUTOMATION OF THE LAGUERRE EXPANSION TECHNIQUE FOR ANALYSIS

OF TIME-RESOLVED FLUORESCENCE SPECTROSCOPY DATA

A Thesis

by

ADITI SANDEEP DABIR

Submitted to the Office of Graduate Studies of
Texas A&M University
in partial fulfillment of the requirements for the degree of

MASTER OF SCIENCE

December 2009

Major Subject: Biomedical Engineering

AUTOMATION OF THE LAGUERRE EXPANSION TECHNIQUE FOR ANALYSIS

OF TIME-RESOLVED FLUORESCENCE SPECTROSCOPY DATA

A Thesis

by

ADITI SANDEEP DABIR

Submitted to the Office of Graduate Studies of
Texas A&M University
in partial fulfillment of the requirements for the degree of

MASTER OF SCIENCE

Approved by:

Chair of Committee:	Javier A. Jo
Committee Members:	Kristen Maitland
	Sebastian Hoyos
Head of Department:	Gerard Cote

December 2009

Major Subject: Biomedical Engineering

ABSTRACT

Automation of the Laguerre Expansion Technique for Analysis of Time-Resolved

Fluorescence Spectroscopy Data.

(December 2009)

Aditi Sandeep Dabir, B.E, University of Pune

Chair of Advisory Committee: Dr. Javier A. Jo

Time-resolved fluorescence spectroscopy (TRFS) is a powerful analytical tool for quantifying the biochemical composition of organic and inorganic materials. The potentials of TRFS as nondestructive clinical tool for tissue diagnosis have been recently demonstrated. To facilitate the translation of TRFS technology to the clinical arena, algorithms for online TRFS data analysis are of great need.

A fast model-free TRFS deconvolution algorithm based on the Laguerre expansion method has been previously introduced, demonstrating faster performance than standard multiexponential methods, and the ability to estimate complex fluorescence decay without any a-priori assumption of its functional form. One limitation of this method, however, was the need to select, a priori, the Laguerre parameter α and the expansion order, which are crucial for accurate estimation of the fluorescence decay.

In this thesis, a new implementation of the Laguerre deconvolution method is introduced, in which a nonlinear least-square optimization of the Laguerre parameter α is performed,

and the selection of optimal expansion order is attained based on a Minimum Description Length (MDL) criterion. In addition, estimation of the zero-time delay between the recorded instrument response and fluorescence decay is also performed based on a normalized means square error criterion.

The method was fully validated on fluorescence lifetime, endogenous tissue fluorophores, and human tissue. The automated Laguerre deconvolution method is expected to facilitate online applications of TRFS, such as clinical real-time tissue diagnosis.

DEDICATION

This thesis is dedicated to my parents, who I can count on to always believe in me and be my constant source of support - in good times and bad. I also dedicate this to my sister for being the wonderful person that she is and for bringing out the all the positive energy in me.

ACKNOWLEDGEMENTS

I would like to thank Dr. Javier Jo, the chair of my advisory committee, for his guidance throughout the duration of my research for this thesis. He has always been available to discuss any issues I had related to my research. His insight has helped me in an immense way to understand the problem better and to take my research forward. His guidance, motivation and encouragement have been the most valuable factors in the completion of this thesis.

I would also like to thank my lab-mates, Chintan, Paritosh and Patrick who have helped in various stages of my research, from providing me with data to being available for any research related discussions and providing constructive suggestions.

Next, I would like to thank my close friends and my cousins here in United States and also those back in India. I thank them for giving me perspective when things looked bleak and for pulling me out of some rough patches.

I once again thank my family, including my extended family for all their good wishes.

TABLE OF CONTENTS

LIST OF FIGURES

Page

LIST OF TABLES

CHAPTER I

INTRODUCTION

Fluorescence spectroscopy has been extensively explored as a technique for detecting biochemical changes in tissue resulting from pathological transformations [1-6]. Tissue autofluorescence is produced by the relative concentration and distribution of endogenous fluorophores. Each fluorophore possesses specific excitation and emission characteristics. Thus, changes in tissue composition will be reflected in the tissue autofluorescence pattern. An extension of the fluorescence spectroscopy method is Time resolved fluorescence spectroscopy (TRFS), which measures the fluorescence intensity emitted by the excited sample as a function of both emission wavelength and time. Thus TRFS records the temporal decay of fluorescence for each wavelength in its emission spectrum. In steady state fluorescence spectroscopy, where only the emission spectrum of the fluorophore is recorded, it might become difficult to distinguish between fluorophores whose emission spectra overlap. Time Resolved Fluorescence provides additional information about the fluorescence dynamics of the sample and can distinguish fluorophores with similar spectra [7].

This thesis follows the style of *IEEE Transactions on Biomedical Engineering*.

1.1 Advantages of using TRFS for biochemical applications

Although steady state fluorescence spectroscopy is simple to implement, it suffers from several disadvantages. There are several biological fluorophores that have emission maxima fairly close to each other indicating that they have overlapping emission spectra[7]. The fluorescence emission intensity measurements depend on several factors such as excitation and collection efficiency, transmission efficiency of optical paths, and optical inhomogeneities in tissues[8-9]. Since steady state measurements are intensity based, it becomes difficult to obtain absolute quantitative measurements that can be correlated to changes in tissue biochemistry. Steady state measurements are also affected by several molecular processes such as photobleaching,[9] quenching,[8] and other diffusive processes occurring in tissues[10].

Time resolved measurements measure the lifetimes of the fluorophores. Time resolved measurements are independent of signal intensity and therefore independent of all artifacts that affect intensity based measurements as mentioned above. Biological components in tissues that emit fluorescence can be identified based on their unique lifetime value regardless of their emission spectra [11-12]. For example, although collagen and elastin are spectrally overlapping, they can be distinguished from each other by their individual lifetime values. Collagen has an approximate lifetime of 1 – 1.5 nanoseconds, whereas elastin has an approximate lifetime of 2 – 2.5 nanoseconds [11-12]. Photobleaching does not cause a change in lifetime, and hence time resolved fluorescence can be applied in spite of a loss in intensity [13]. Quenching can be monitored advantageously using time resolved measurements to understand molecular

mechanisms as changes in lifetime are proportional to the rate of quenching processes[14]. Thus time resolved fluorescence spectroscopy can be a powerful tool for clinical applications in tissues since it is more robust as compared to steady state fluorescence spectroscopy and can provide more information.

TRFS can detect the presence and estimate the concentration of intrinsic fluorophores like elastin, collagen which determine the structural properties of human tissue, and enzyme cofactors (NADH, FAD) which reflect the biochemical composition of the tissue. This offers potential to probe the structural and biochemical properties of the tissue and hence detect any tissue abnormalities [15]. TRFS has already been evaluated as a tool for in-vivo analysis of tissue for clinical diagnosis [2-6, 15-16]. A significant challenge in clinical application of TRFS that still needs to be addressed is the development of robust and automated computational methods for analysis of TRFS data.

1.2 Data analysis of TRFS

Time resolved fluorescence spectroscopy works with the assumption that the excitation pulse is an impulse (δ) function. In such a case, the measured fluorescence decay will be the fluorescence Impulse Response Function (IRF). However, in most practical cases the excitation laser pulse has a finite width. Hence the measured data is thus more accurately described as a convolution function of the IRF and the instrument response.

$$y(n) = T \sum_{m=0}^{K-1} h(m)x(n-m); \qquad n = 0,1,...K-1$$

(1)

where $y(n)$ is the measured fluorescence decay, $x(n)$ is the instrument response and $h(n)$ is the fluorescence IRF. The instrument response is generally estimated as the laser pulse recorded as scattered by the sample. The IRF contains all the information about the fluorescence dynamics and hence composition of the fluorophore; hence it is essential to isolate it from the instrument response using deconvolution.

1.2.1 Standard methods

A number of methods have been used for the problem of deconvolution, the most common among them being the Least Square Iterative Reconvolution (LSIR). It uses a multiexponential model which assumes the fluorescence IRF to be a summation of exponential terms with different decay constant and coefficients. The decay constants and coefficients are found using the method of LSIR. [17],[18] Multiexponential method does not always converge to the same solution. Several solutions may exist for the same data if this model is used. Moreover, this model is insufficient for clinical application because a limited number of decay times cannot account for the fluorescence dynamics of the entire biological environment of the tissue [7, 19]. For such a complex medium, the multiexponential functions cannot be interpreted in terms of fluorophore content or number of lifetime components. Thus, for tissue analysis, it is advantageous to avoid making any a priori assumption of functional form of the IRF.

1.2.2 Laguerre Expansion Technique

More recently, the Laguerre Expansion Technique (LET) has been used for deconvolution, which is faster and more accurate than the more widely used current

methods [13]. LET was adapted and popularized in the early 1990s by Marmarelis for linear and non-linear modeling[12] [20]. This method has been extensively applied since then to the modeling of different physiological systems, including renal autoregulation and cardiac autonomic control [21-22]. Taking advantage of the asymptotically declining nature of the Discrete Laguerre Functions (DLFs), the LET was more recently adapted for the deconvolution of TRFS decay data and estimation of fluorescence IRFs [23-24]. This technique models the fluorescence decay using an orthonormal Laguerre basis formed by the DLFs, thus making it possible to accurately express the fluorescence decay by a finite number of terms in the expansion (usually 3 to 7). In addition, the Laguerre expansion coefficients can be further analyzed to estimate the relative concentration of fluorophores in complex fluorescence systems. They can also be used as features while developing classification algorithms to perform TRFS based tissue diagnosis [2-3, 23, 25].

However, the Laguerre deconvolution method in its present form is inadequate for the application of TRFS in clinical diagnosis since it still requires the proper selection of the correct Laguerre parameter, α, which can vary depending on the temporal behavior of the fluorescence decay [12, 26] . The Laguerre parameter α takes values between 0 and 1 and it determines the rate of exponential decline of the Laguerre functions [20]. For a smaller alpha, the Laguerre functions decay faster, while for a larger alpha the DLFs have slower declining rate. Thus, while modeling the fluorescence IRF using DLFs, fluorophores with lower lifetime generally require smaller α while a larger α value may be required for expanding long-lived fluorescence decays. Another challenge with Laguerre Expansion

Technique is the selection of the optimal expansion order for the Laguerre functions. The expansion order indicates the number of Laguerre functions needed for accurate modeling of the fluorescence decay. In general, more DLFs (i.e. higher order ones) are needed to expand complex decay dynamics. In such a case if too few DLFs are used, they might be insufficient to completely express the complex fluorescence decay. On the other hand, too many DLFs in the expansion can cause model over fitting, in which case the model might end up tracking noise and any trends that might be present in the signal which do not contribute to any information about the fluorescence dynamics. Thus the selection of the optimal order has to be done so as to achieve maximum goodness of fit while avoiding over-fitting, and finding a suitable tradeoff between accuracy and computation time.

Selection of both the Laguerre parameter and the expansion order has so far been done by trial and error methods[2-3, 23, 25], which are not suitable for fast on-line analysis of TRFS data.

1.3 Zero time-delay

There is another issue with TRFS measurements described as the 'zero-time delay'. Ideally the instrument response should be measured at the same wavelength as the emission fluorescence in order to minimize any wavelength dependent distortion of the instrument response introduced at the detector or transmission medium. In practice, however, the instrument response is recorded as the scattered light at the excitation wavelength. Since the excitation has a shorter wavelength than the emission, it travels

through the fiber much slower than the fluorescence, which is in the visible range for most tissue fluorophores. This introduces a delay between the recorded instrument response and the fluorescence. This delay depends on the optical path length and the wavelength at which the fluorescence is measured. The estimation and adjustment of this delay is necessary before any further analysis about the fluorescence decay is done.

In this thesis, a new implementation of the Laguerre deconvolution method for fluorescence IRF estimation is introduced. This new automated Laguerre deconvolution approach performs a nonlinear least-square optimization of the Laguerre parameter alpha, finds the optimal expansion order based on Minimum Description Length (MDL) criterion, and corrects for the zero-time delay between the recorded instrument response and fluorescence decay based on a normalized means square error criterion. Results of the method validation on synthetic data, fluorescence standard measurements and biological tissues are presented. Unlike its previous implementations, the automated Laguerre deconvolution method converges to an accurate fluorescence IRF and lifetime estimation without the need for choosing a priori the expansion parameters, making it more suitable for online analysis and real-time applications, such as tissue diagnosis based on TRFS and fluorescence lifetime imaging.

CHAPTER II

BACKGROUND

Before we can proceed to analyze the time resolved fluorescence spectroscopy data, it is important to understand the physical process of fluorescence at the molecular level and the factors that affect the nature of the fluorescence decay. This section will cover fluorescence photophysics, background of fluorescence spectroscopy, introduction to frequency domain TRFS and in some more detail, time domain TRFS.

2.1 Fluorescence photophysics

When a molecule is excited to a higher energy level, it returns to the ground state resulting in emission of radiation. This phenomenon is called luminescence. The energy associated with the emitted radiation is equal to the difference between the excited and ground state energy levels. If the excited state is a singlet state, the excited electron has spin that is opposite to the electron in the ground state. In this condition it is easier for the electron to return to the ground state and hence the process of emission is very fast. In this case, the emission is called fluorescence and it has small decay times of the order of 10 ns [7]. If the excited stat is a triple state, however, the electron in the excited state has the same spin as the electron in the ground state. Transitions from such a state to the ground state are forbidden and in such cases the decay times can be very large (of the order of 10^3 seconds). This phenomenon is called phosphorescence. This thesis will be focusing on fluorescence.
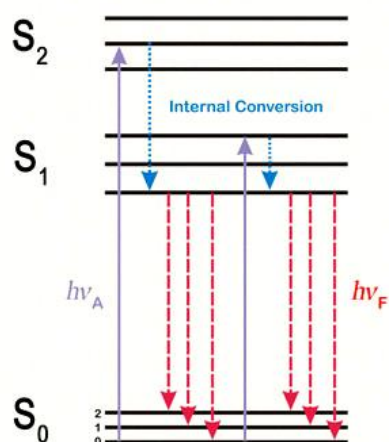
Figure 1. Jablonski Diagram [44]

The Jablonski diagram (Figure 1) will now be used to explain the process of fluorescence in more detail. S0, S1 and S2 denote the singlet electronic states of the molecule. Each electronic energy state is associated with several vibrational energy states. Before being excited the electron is present in the lowest vibrational state of the S0 electronic energy level. It is excited to any of the higher electronic levels, say using a laser, (either S1 or S2, depending on the energy of excitation, i.e. the laser wavelength) and to any of the several vibrational states associated with that electronic level. The fact that it can be excited to any of these vibrational levels is what causes the characteristic excitation spectrum for the molecule. Before returning to the ground state, the electron must occupy the lowest vibrational state of the electronic level in which it has been present. The process by which the electron transitions to this state is accompanied with an energy loss but is non radiative and is called internal conversion. The photon emitted after internal conversion has lower energy and hence longer wavelength than the photon that was

absorbed. This difference in energy or a difference in wavelength between the absorbed and emitted photon is known as Stokes shift [7].

After internal conversion, the electron returns to the ground state, but it can do so at any of the vibrational levels associated with the ground state. This gives rise to a characteristic emission spectrum which is a reflection of the distribution of vibrational levels in the ground state of the entire molecular species. The fluorescence intensity of a molecule is characterized by several properties such as the molar extinction coefficient (i.e. the absorbing power) at the excitation wavelength, quantum yield (ratio of number of photons emitted to the number absorbed) at the emission wavelength and the concentration of the molecule in solution [7].

2.2 Fluorescence decay kinetics

The fluorescence lifetime is defined as the average time that a molecule spends in the excited state before decaying to the ground state by emitting photons. Fluorescence emission is a random process and not all molecules stay in the excited state for the same amount of time.

After a sample is excited with an infinitely short pulse of light, a certain population of the sample (say n_o) is excited to a higher energy level. This population begins to decay into the ground state with a rate $\Gamma + knr$.

$$(dn(t))/dt = (\Gamma + k_{nr})n(t) \tag{2}$$

where $n(t)$ is the number of molecules in the excited state at the instant t. Since emission is a random event, each molecule in the sample has the same probability of emitting in a

given period of time. Hence after having excited a sample, the process by which all the molecules in the sample return to the ground state forms an exponential decay. Since the fluorescent intensity corresponds to the number of emitting molecules,

$$I(t) = I_0 \, exp(-t/\tau) \tag{3}$$

where I_0 is the intensity at time $t = 0$. The lifetime is the inverse of the total decay rate. That is,

$$\tau = (\Gamma + k_{nr})^{-1} \tag{4}$$

Thus, lifetime is defined as the rate of the exponential decay of fluorescence emission with time [7].

2.3 Fluorescence spectroscopy

The interaction of light with matter can result in several processes such as scattering, reflection, absorption and luminescence. Hence measurement of these processes at a molecular level can help identify the sample's molecular structure and chemistry. Optical spectroscopy has been used as a tool to study these processes over a range of wavelengths and define a spectrum over which the sample under investigation is active [7, 9, 27]. Steady state fluorescence spectroscopy primarily consists of exciting the sample with a wavelength in the sample's excitation/absorption spectrum and measuring the intensity over the emission spectrum. Time resolved spectroscopy involves collecting information about temporal fluorescence dynamics for each wavelength in the emission spectrum. Time Resolved Fluorescence Spectroscopy can be performed in time domain or frequency domain. In frequency domain the excitation source used is a continuous wave source (see figure 3 on page 22). It is intensity modulated at a high frequency that is

comparable to the reciprocal of lifetime. The resulting emission intensity is also modulated at the same frequency. However the emission intensity signal is not exactly the same as the excitation signal but is characterized by time-delay and amplitude changes compared to the excitation signal. The time delay is measured as the phase shift between the excitation and emission signal [7, 28].
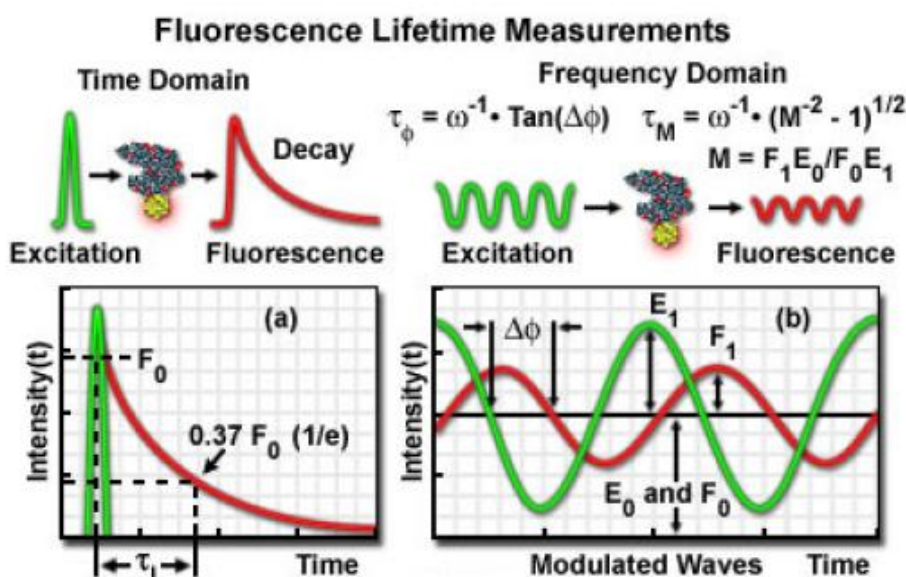
Figure 2. Time domain and frequency domain TRFS [45]

2.4 Time resolved fluorescence spectroscopy (Time domain)

In time domain time resolved fluorescence spectroscopy the sample is excited by a very narrow pulse of light (Figure 2). The width of the pulse is preferably much narrower than the expected fluorescence lifetime of the sample (ideally, an impulse function). The resulting emission intensity is collected as a time dependent signal at each wavelength in the spectrum. The fluorescence signal in this case is asymptotically decaying and this signal is a characteristic of the particular fluorophore[7]. There are several approaches

that can be used to implement time domain time resolved fluorescence spectroscopy. Although a pulsed laser is invariably used as an excitation source, different detection and acquisition schemes can be used according to the application. Time Correlated Single Photon Counting (TCSPC)[29], high speed time gated CCD devices[30-31], streak cameras[31] and pulse sampling/transient recording through a high speed digitizer[32] are some of the time domain approaches that can be employed. Time correlated single photon counting (TCSPC) works on the principle that a single photon is detected for more than one excitation pulse. The delay time between that excitation pulse and the detection of the first photon is recorded. Each of these photons detected are stored in a histogram with the horizontal axis representing the delay between excitation pulse and detection of the first photon and the vertical axis representing the photon count at that specific delay interval. When a sufficient amount of photons (of the order of 10^6) have been recorded in the histogram, it will represent the recorded decay [29]. Pulse sampling or transient recording is another approach that has recently gained popularity for time resolved fluorescence spectroscopy in clinical applications. It allows recording of an entire decay with a single excitation pulse at a good signal to noise ratio. High speed digitizers or digital oscilloscopes can be used for the purpose of decay pulse sampling. High bandwidth detectors are used to record fluorescence intensity decay over time. With the advent of high speed digitizers and advanced MCP-PMTs, systems with high temporal and spectral resolution have been developed[32].

CHAPTER III

METHODS

In this section, the automated Laguerre deconvolution method will be presented. Then, a description of the experiments performed for validating the proposed deconvolution method and comparing it with other more standard ones will be provided.

3.1 Automated Laguerre deconvolution technique

3.1.1 Basic Laguerre Expansion Technique for deconvolution of TRFS data

In the context of TRFS, the measured fluorescence intensity decay data $y(n)$ is given by the convolution of the fluorescence IRF $h(n)$ with the instrument response $x(n)$,

$$y(n) = T \sum_{m=0}^{K-1} h(m)x(n-m);$$

(5)

The parameter K in equation (5) determines the time length of the fluorescence IRF and T is the sampling interval. The Laguerre deconvolution technique expands the fluorescence IRF on an orthonormal set of discrete time Laguerre functions (DLF) $b_j^\alpha(n)$,

$$h(n) = T \sum_{j=0}^{L-1} c_j^\alpha b_j^\alpha(n)$$

(6)

In equation (6), c_j^α are the unknown Laguerre expansion coefficients (LEC), which are to be estimated from the input-output data; $b_j^\alpha(n)$ denotes the jth order orthonormal DLF;

L is the number of DLFs used to model the IRF, thus defining the order of the expansion. The DLF of order j is defined as,

$$b_j^n(n) = \alpha^{\frac{n-j}{2}}(1-\alpha)^{\frac{1}{2}}\sum_{k=0}^{j}(-1)^k \binom{n}{k}\binom{j}{k}\alpha^{j-k}(1-\alpha)^k; \quad n \geq 0$$

(7)

The order j of each DLF is equal to its number of zero-crossing (roots). The Laguerre parameter α ($0 < \alpha < 1$) determines the rate of exponential (asymptotic) decline of the DLFs. The higher the order j and/or the larger the Laguerre parameter α, the longer the spread over time of a DLF and the larger the time separation between zero-crossing. Thus, higher order and larger α value imply longer convergence time to zero. By inserting equation (6) into equation (5), the convolution equation (5) becomes,

$$y(n) = \sum_{j=0}^{L-1} c_j^\alpha v_j^\alpha(n)$$

(8)

Where the functions $v_j^\alpha(n)$, represent the digital convolution of the input x(n) with each of the Laguerre functions, are denoted as the "key variables".

$$v_j^\alpha(n) = \sum_{m=0}^{L-1} b_j^\alpha(m)x(n-m);$$

(9)

The computation of $v_j^\alpha(n)$ can be accelerated significantly by use of the recursive relation

$$v_j^\alpha(n) = \sqrt{\alpha}v_j^\alpha(n-1) + \sqrt{\alpha}v_{j-1}^\alpha(n) - v_{j-1}^\alpha(n-1)$$

(10)

which is due to the particular form of the discrete-time Laguerre function [12]. Computation of this recursive relations must be initialized by the following recursive equation that yield $v_0^\alpha(n)$ for a given input $x(n)$,

$$v_0^\alpha(n) = \sqrt{\alpha}v_0^\alpha(n-1) + \sqrt{(1-\alpha)}\,x(n-1) \tag{11}$$

The system of linear equation (8) can be expressed in a matrix notation as follows,

$$\underbrace{\begin{bmatrix} y(0) \\ y(1) \\ \vdots \\ y(N-1) \end{bmatrix}}_{\bar{y}[N\times1]} = \underbrace{\begin{bmatrix} v_0^\alpha(0) & v_1^\alpha(0) & \dots & v_{L-1}^\alpha(0) \\ v_0^\alpha(1) & v_1^\alpha(1) & \dots & v_{L-1}^\alpha(1) \\ \vdots & \vdots & \ddots & \vdots \\ v_0^\alpha(N-1) & v_1^\alpha(N-1) & \dots & v_{L-1}^\alpha(N-1) \end{bmatrix}}_{V_\alpha[N\times L]} \underbrace{\begin{bmatrix} c_0^\alpha \\ c_1^\alpha \\ \vdots \\ c_{L-1}^\alpha \end{bmatrix}}_{\bar{c}_\alpha[L\times1]}$$

$$\tag{12}$$

Equation (12) can be written as

$$\bar{y} = V_\alpha \bar{c}_\alpha \tag{13}$$

The least-square analytical solution for (13) is given as,

$$\hat{c}_\alpha = (V_\alpha^T V_\alpha)^{-1}V_\alpha^T\bar{y} \tag{14}$$

Hence the estimated decay can be expressed as,

$$\hat{y} = V_\alpha(V_\alpha^T V_\alpha)^{-1}V_\alpha^T\bar{y} \tag{15}$$

Where the inversion is performed using a QR decomposition. Once the expansion coefficients $\bar{c}_\alpha$ have been calculated, the fluorescence IRF $h(n)$ can be computed from (6), the estimated fluorescence decay $\hat{y}_\alpha(n)$ can be found by convolving the input with $h(n)$ (the subscript α defines the specific Laguerre basis used for the expansion), and values for average lifetimes can be calculated as [7],

$$\tau = \frac{T \cdot \sum_{n=0}^{N}[n \cdot h(n)]}{\sum_{n=0}^{N}[h(n)]}$$

$$\tag{16}$$

3.1.2 Non-linear least square optimization of the Laguerre parameter

The choice of the Laguerre parameter α is critical in achieving accurate fluorescence IRF expansions. As a first approach, the parameter α can be selected based on the kernel memory length K and the number of DLFs used for the expansion, so that all the functions converge to zero by the end of the impulse response [20, 26]. However, this empirical approach does not warranty an optimal expansion, and in practice, a good choice for the value of α is usually found by trial-and-error procedures. Here, we propose a computationally efficient method, whereby the Laguerre parameter is treated as a free parameter within a nonlinear least-square optimization scheme. This automates the procedure for the determination of suitable Laguerre parameters, guided by the actual TRFS experimental data.

In the context of nonlinear least square optimization, the model free parameter (α in this case) is chosen so that an objective function is minimized. The objective function $F(\alpha)$ is defined as the sum of squared errors (ε_N) between the measured fluorescence decay $\bar{y}(n)$ and its estimation $\hat{y}_\alpha(n)$,

$$F(\alpha) = \varepsilon_N^T \varepsilon_N \; ; \quad \varepsilon_N = \bar{y}(n) - \hat{y}_\alpha(n) \tag{17}$$

The optimal alpha is selected as,

$$\hat{\alpha} = argmin_\alpha F(\alpha) \tag{18}$$

To minimize the objective function, the Laguerre parameter is iteratively updated,

$$\hat{\alpha}^{k+1} = \hat{\alpha}^k - \gamma^k \left[\frac{d(F(\alpha))}{d\alpha}\right]^k \tag{19}$$

Where the superscript k denotes the iteration number and γ is a scaling factor chosen so that the Laguerre parameter is updated by a fixed amount after each iteration. Estimation

of $\frac{d(F(\alpha))}{d\alpha}$ can be performed by numerical methods. Alternatively, closed from recursive

formulation of $\frac{d(F(\alpha))}{d\alpha}$ can also be derived as follows,

We use Eq. (14) to express the estimation error ε_N, as,

$$\varepsilon_N = \bar{y} - \hat{y} = \bar{y} - V_\alpha (V_\alpha^T V_\alpha)^{-1} V_\alpha^T \bar{y} \tag{20}$$

Substituting for ε_N from Eq. (20) into Eq. (17), we get,

$$F(\alpha) = (\bar{y} - V_\alpha (V_\alpha^T V_\alpha)^{-1} V_\alpha^T)^T (\bar{y} - V_\alpha (V_\alpha^T V_\alpha)^{-1} V_\alpha^T) \tag{21}$$

This can be further simplified to,

$$F(\alpha) = \bar{y}^T (I_N - V_\alpha (V_\alpha^T V_\alpha)^{-1} V_\alpha^T)^T \bar{y} = \bar{y}^T (\bar{y} - V_\alpha (V_\alpha^T V_\alpha)^{-1} V_\alpha^T \bar{y}) \tag{22}$$

Where I_N is the identity matrix or order N. By identifying the second term on the RHS as

ε_N, we get,

$$F(\alpha) = \bar{y}^T \varepsilon_N \tag{23}$$

Thus, the derivative of the cost function can simply be expressed as,

$$\frac{d(F(\alpha))}{d(\alpha)} = \bar{y}^T \frac{d(\varepsilon_N)}{d(\alpha)} \tag{24}$$

Using the definition of ε_N from Eq. (20), it derivative with respect to α beomes,

$$\frac{d(\varepsilon_N)}{d(\alpha)} = \frac{d(\bar{y} - V_\alpha \hat{c}_\alpha)}{d(\alpha)} = -\frac{d(V_\alpha \hat{c}_\alpha)}{d(\alpha)} = -\left[\frac{d(V_\alpha)}{d(\alpha)} \hat{c}_\alpha + V_\alpha \frac{d(\hat{c}_\alpha)}{d(\alpha)} \right] \tag{25}$$

The key variables $v_j^\alpha(n)$ can be computed recursively as shown in Eq. (10) and Eq. (11)

[26].

Using this, we can derive a recursive formulation for the terms in $\frac{dV_\alpha}{d\alpha}$, where V_α is the

matrix formed by the key variables.

Recursive estimation of $\frac{dv_j^\alpha(n)}{d\alpha}$ can be derived by taking the derivative of Eq. (5) and (6)

with respect to α, yielding the following set of equations,

$$\frac{dv_j^\alpha(n)}{d\alpha} = \frac{1}{2\sqrt{\alpha}} \left(v_j^\alpha(n-1) + v_{j-1}^\alpha(n) \right) + \sqrt{\alpha} \left(\frac{dv_j^\alpha(n-1)}{d\alpha} + \frac{dv_{j-1}^\alpha(n)}{d\alpha} \right) - \frac{dv_{j-1}^\alpha(n)}{d\alpha}$$

$$\frac{dv_0^\alpha(n)}{d\alpha} = \frac{1}{2\sqrt{\alpha}} \left(v_j^\alpha(n-1) \right) + \sqrt{\alpha} \left(\frac{dv_j^\alpha(n-1)}{d\alpha} \right) + \frac{1}{2\sqrt{1-\alpha}} \, x(n)$$

(26)

Similarly, by taking the derivative with respect to the least square solution of the

expansion coefficients as defined in Eq. (6), we obtain,

$$\frac{d(\hat{c}_\alpha)}{d(\alpha)} = \frac{d(V_\alpha^T V_\alpha)^{-1} V_\alpha^T \bar{y})}{d(\alpha)} = \frac{d((V_\alpha^T V_\alpha)^{-1})}{d(\alpha)} V_\alpha^T \bar{y} + (V_\alpha^T V_\alpha)^{-1} \frac{d(V_\alpha^T \bar{y})}{d(\alpha)}$$

(27)

To calculate $\frac{d((V_\alpha^T V_\alpha)^{-1})}{d(\alpha)}$ let us first consider that,

$$\frac{d((V_\alpha^T V_\alpha)^{-1}(V_\alpha^T V_\alpha))}{d(\alpha)} = \frac{d((V_\alpha^T V_\alpha)^{-1})}{d(\alpha)} V_\alpha^T V_\alpha + (V_\alpha^T V_\alpha)^{-1} \frac{d(V_\alpha^T V_\alpha)}{d(\alpha)}$$

Since $(V_\alpha^T V_\alpha)^{-1}(V_\alpha^T V_\alpha) = I_N$, the LHS becomes zero, thus,

$$\frac{d((V_\alpha^T V_\alpha)^{-1})}{d(\alpha)} = (V_\alpha^T V_\alpha)^{-1} \frac{d(V_\alpha^T V_\alpha)}{d(\alpha)} (V_\alpha^T V_\alpha)^{-1}$$

(28)

Substituting Eq. (14) in Eq. (28), we get,

$$\frac{d(\hat{c}_\alpha)}{d(\alpha)} = (V_\alpha^T V_\alpha)^{-1} \left\{ \frac{dV_\alpha^T}{d(\alpha)} \bar{y} - \left[\frac{dV_\alpha^T}{d(\alpha)} V_\alpha + V_\alpha^T \frac{dV_\alpha}{d(\alpha)} \right] \hat{c}_\alpha \right\}$$

(29)

$$\frac{d(F(\alpha))}{d(\alpha)} = \bar{y}^T \left\{ \frac{dV_\alpha}{d\alpha} \hat{c}_\alpha + V_\alpha (V_\alpha^T V_\alpha)^{-1} \left[\frac{d(V_\alpha^T)}{d\alpha} \bar{y} - \left(\frac{d(V_\alpha^T)}{d\alpha} V_\alpha + V_\alpha^T \frac{dV_\alpha}{d\alpha} \right) \hat{c}_\alpha \right] \right\}^{(k)}$$

(30)

Finally the iterative relation for calculation the optimal Laguerre parameter becomes,

$$\hat{\alpha}^{k+1} = \hat{\alpha}^k + \gamma^k \bar{y}^T \left\{ \frac{dV_\alpha}{d\alpha} \hat{c}_\alpha + V_\alpha (V_\alpha^T V_\alpha)^{-1} \left[\frac{d(V_\alpha^T)}{d\alpha} \bar{y} - \left(\frac{d(V_\alpha^T)}{d\alpha} V_\alpha + V_\alpha^T \frac{dV_\alpha}{d\alpha} \right) \hat{c}_\alpha \right] \right\}^k$$

(31)

where the derivatives of the key variables are given by Eq. (26). Iterative updating of the

Laguerre parameter α is performed using until a nonlinear least square optimal solution is

attained.

3.1.3 Expansion order selection

The deconvolution approach based on the Laguerre expansion technique can be taken as an identification problem, in which the model complexity (i.e. number of Laguerre functions for the expansion) are to be determined. Increasing the model complexity will decrease the systematic errors. However, at a certain complexity, additional model parameters no longer reduce the systematic errors but are used to follow the actual noise realization on the data, a phenomenon known as overfitting. To avoid this unwanted behavior, a model selection criterion usually includes a model complexity term to penalize overfitting conditions. Among the various model selection criterion used, one of the most robust and commonly used ones is the minimum description length (MDL) index[33-34], which is defined as follows [33, 35]

$$MDL(L) = \frac{F(\alpha)}{N} exp\left(\frac{ln(N) \cdot L}{N}\right) \tag{32}$$

Here, N is the number of measured samples, $F(\alpha)$ is the sum of squared errors as defined in (10), and L is the number of model parameters, which in this case corresponds to the number of Laguerre functions used for the expansion. To estimate the optimal expansion order, L takes values from 2 to 8, and $MDL(L)$ is computed. The value of L that yields the minimum $MDL(L)$ value is then chosen as the optimal expansion order.

3.2 Zero-time delay estimation

As discussed before, when the instrument response is recorded experimentally as the scattering of the excitation light pulse, a zero-time shift or delay of the instrument response with respect to the fluorescence decay is often observed. Here, we describe a heuristic method for accurate estimating such delay between the scattered based instrument response and fluorescence emission decay. Basically, a number of potential

delays between the instrument response and the fluorescence decay are assumed. For each delay value, the Laguerre deconvolution is applied using a fixed order of 4, and the normalized means-square error (NMSE) values is computed. Then, the delay yielding the lowest NMSE is taken as the optimal delay between the instrument response and the analyzed fluorescence decay at a given emission wavelength.

3.3 Method validation experimental TRFS data

The performances of the automated Laguerre deconvolution technique was assessed with experimental TRFS data from lifetime fluorescence standards and human ex-vivo arteries. A brief description of the fluorescence measurements is presented here.

3.3.1 TRFS instrumentation

The experiments for validation were conducted with a TRFS system, built on the lines of a first prototype [32]. The fluorescence standard samples were excited with a subnanosecond pulsed nitrogen laser with emission wavelength 337.1 nm (700 ps FWHM). The fluorescence response was measured using a customized TRFS system allowing for direct recording of the fluorescent pulse (fast digitizer and gated detection). Fluorescence pulse was collected by a fiber optic bundle (bifurcated probe) and directed to a monochromator connected to a multi-channel plate photo-multiplier tube (transit time spread of 90 ps). The entire fluorescence pulse from a single excitation pulse was recorded with a 2.5 GHz bandwidth digital oscilloscope (Sampling rate, 10Gsamples/s) coupled to a preamplifier (bandwidth 1.5 GHz). For each sample solution, the fluorescence decay corresponding to the peak emission wavelength of that fluorophore was recorded. After the fluorescence measurement, the scattered laser pulse temporal

profile was measured at a wavelength slightly below the excitation laser line. The laser pulse energy at the tip of the excitation fiber probe was adjusted to 5.0 µJ/pulse.

3.3.2 Experimental data, fluorescence lifetime standards and fluorescent tissue constituents

Data was collected from standard dyes for fluorescence lifetime measurements. The fluorescence lifetime standards were selected to cover a broad range of emission wavelengths (360–650) nm and radiative lifetimes (0.4–12 ns). The fluorophores used were rose Bengal (33,000, Sigma-Aldrich), Rhodamin B (25,242, Sigma-Aldrich), and 9-cyanoanthracene (15,276, Sigma-Aldrich). These fluorophores are commercially available in powder form. The fluorescence dyes used in the measurements were diluted into 10^{-6} M solutions.
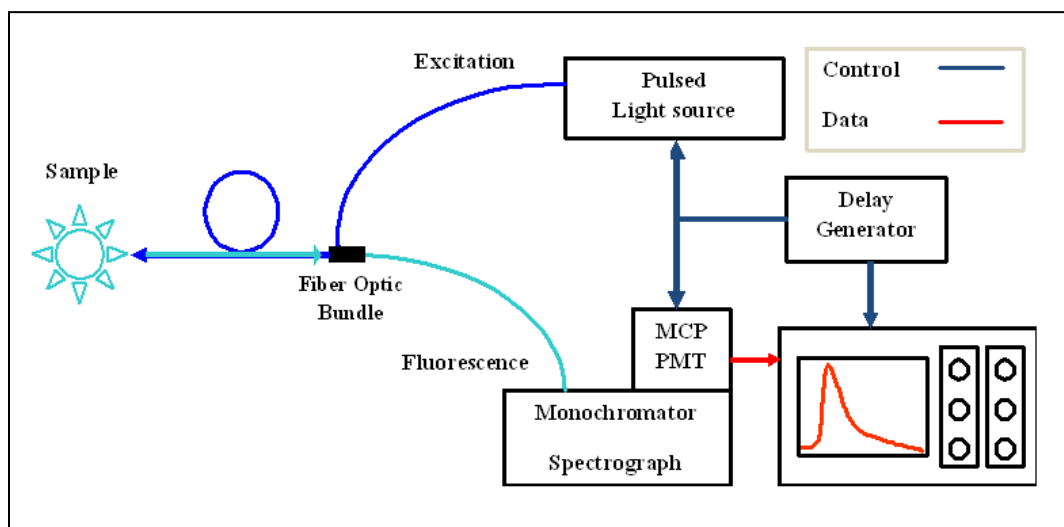

Figure 3. Block diagram of TRFS instrumentation.

In addition to fluorescence lifetime standard, the deconvolution method was also evaluated on fluorescent tissue constituents tested, relevant for potential fluorescence

based tissue diagnosis [36-37]. These include commercially available samples of collagen type I (C3511, Sigma-Aldrich), NADH (N8129, Sigma-Aldrich), and flavin adenine dinucleotide (FAD) disodium salt dihydrate (F6625, Sigma-Aldrich). The collagen was tested in dry form while NADH and FAD were tested in 10^{-6} M PBS solutions. The time-resolved fluorescence decays of these specimens were obtained in the same manner as the fluorescence standard dyes.

3.3.3 Experimental data, TRFS ex-vivo measurement from human arteries

Finally, the automated Laguerre deconvolution method was also tested on TRFS measurements obtained from human tissue. An important future possibility for method is for enabling application of TRFS as a clinical tool to detect biochemical composition on atherosclerotic arteries, we used human coronary arteries (postmortem specimens) for this validation study. In this case, the time-resolved fluorescence spectra were measured for a 200 nm spectral range from 400 nm to 650 nm at 5 nm increments. Spectra were acquired from several locations from the lumen side within the coronary arteries. The scattered laser pulse temporal profile was also measured right after each time-resolved fluorescence spectrum acquisition. The laser pulse energy at the tip of the excitation fiber probe was also adjusted to 5.0 μJ/pulse.

3.4 Comparison with standard deconvolution method

In order to compare the deconvolution performance of the proposed method with more standard approaches, we also analyzed the same TRFS data using the standard multiexponential least-square iterative reconvolution (LSIR) approach. LSIR applies

nonlinear least-square optimization methods to estimate the parameters of a multi-exponential IRF that would fit best its convolution with the instrument response with the fluorescence decay data. For the data considered in this study, up to three exponential components were assumed.

CHAPTER IV

RESULTS

4.1 Validation on fluorescence lifetime standards and fluorescent tissue constituents

The proposed automated deconvolution method was first validated on TRFS measurements from fluorescence lifetime standards. Results for this first validation are summarized in Figure 4 and Table 1. Figure 4 shows the standard fluorescence pulse measured at their peak emission wavelength, together with the instrument response, and the estimated fluorescence pulses by the automated Laguerre and the multiexponential deconvolution methods. The estimated fluorescence IRF, the normalized residuals, and the autocorrelation of the residuals are also shown. To assess the ability of the Laguerre technique to estimate long fluorescence lifetimes, the fluorescence decay of 9-cyanoanthracene (9CA) in ethanol were deconvolved (Figure 4.a-b). Both the Laguerre and the exponential methods yielded similar fluorescence IRFs with lifetime values in agreement with previous reports[7, 32, 38-39] (Table 1). The normalized residuals (<10%) and their autocorrelation functions show a significantly random   behavior, indicating excellent performance by the two methods.

Optimal values of α=0.96 and order L=4 were obtained, and two exponential components were needed for proper multiexponential deconvolution. Similarly, measurements of Rhodamin B in ethanol demonstrated the ability of the automated Laguerre method to accurately resolve nanosecond fluorescence lifetimes (Figure 4.c-d). Again, both methods yielded similar fluorescence IRFs with lifetime values also in agreement with previously reported (Table 1), and the excellent estimation accuracy was also evident by the low normalized residual (<5%) and flat autocorrelation function. . For this case, optimal values of α=0.84 and order L=4 were obtained, and two exponential components were needed for proper multiexponential deconvolution. Short-lived fluorescence IRF, like that from Rose Bengal in ethanol, with lifetimes ranging in the hundreds of picoseconds could be also reliably retrieved by the proposed deconvolution technique (Figure 4.e-f). Optimal values of α=0.57 and order L=3 were obtained, and two exponential components were used for this fluorophore. As in the previous cases, both methods yielded similar fluorescence IRFs with lifetime values in agreement with those reported in the literature[7, 32, 39] (Table 1).
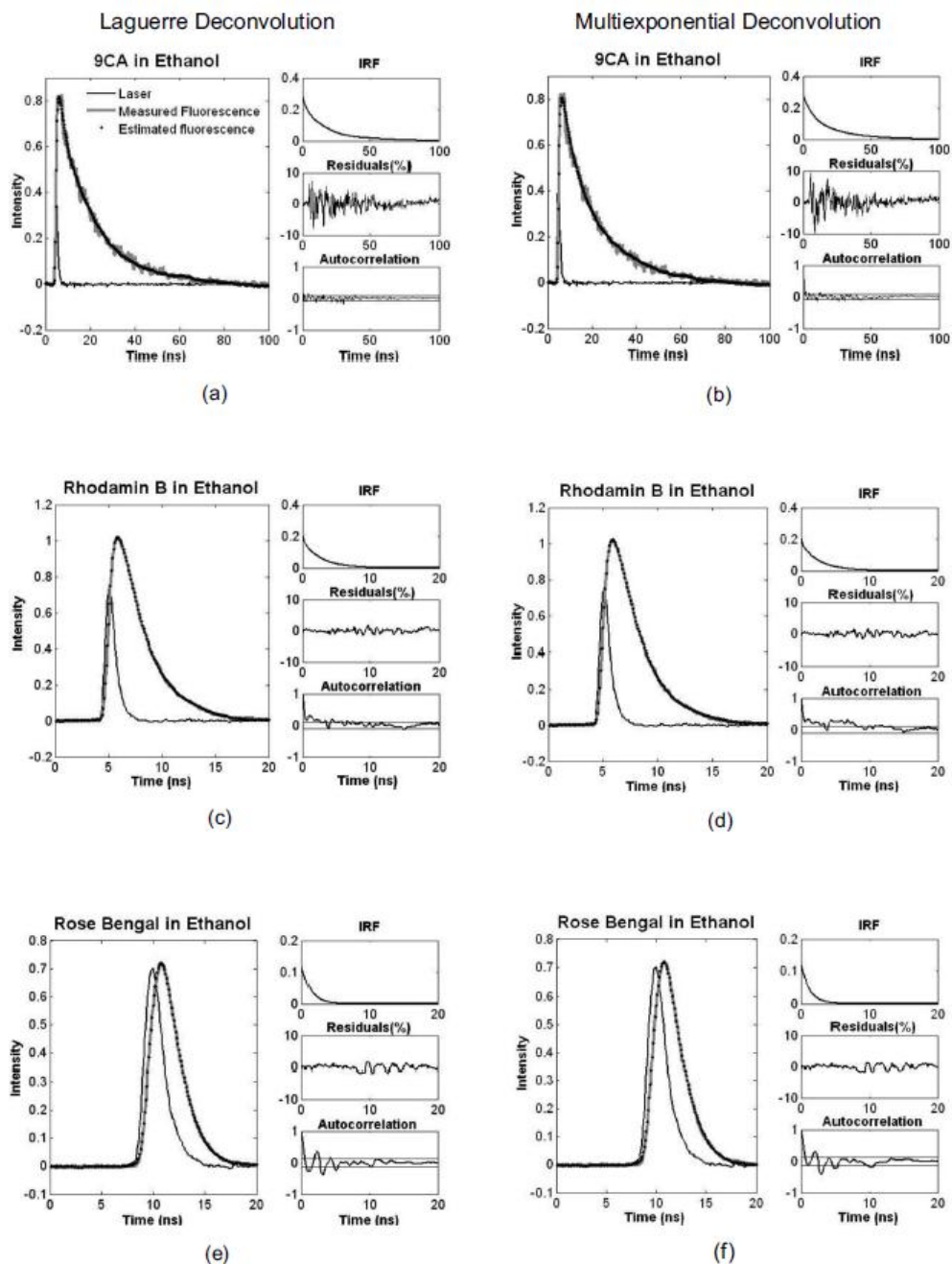
Figure 4. Deconvolution results for TRFS data from fluorescence lifetime standards (a) and (b), 9CA at 450nm, (c) and (d), Rhodamin B at 580 nm and (e) and (f) Rose Bengal at 570 nm using the Automated Laguerre (left and multiexponential (right) methods. Main panels show the measured fluorescence pulse (solid black), instrument response (solid gray), and estimated fluorescence pulse (dotted black). Smaller panels show the Fluorescence IRF (top), normalized residuals (middle) and residual autocorrelation (bottom). The fluorescence IRFs were accurately estimated by both methods

Following the validation with fluorescence lifetime standards, TRFS data was measured and analyzed from three important tissue constituents relevant for potential fluorescence based tissue diagnosis, collagen, NADH and FAD. Results for this second validation are summarized on Figure 5 and Table 1. Both the automated Laguerre and multiexponential methods accurately estimated the collagen fluorescence IRF and lifetime values at its peak emission wavelength of 400 nm, as shown in Figure 5.a-b and Table 1. From the residuals plots however, it seemed that the Laguerre approach performed better (<5% error) than the multiexponential deconvolution (<10% error). Optimal values of $\alpha=0.91$ and order L=3 were obtained, and two exponential components were needed for proper multiexponential deconvolution. The NADH fluorescence IRF and lifetime value at the peak emission of 450 nm were also properly estimated by both methods, as reflected in Figure 5.c-d and Table 1. For this fluorophore, optimal values of $\alpha=0.67$ and order L=4 were obtained, and two exponential components were used. Similarly, both methods accurately estimated the fluorescence IRF and lifetime of FAD (Figure 5.e-f) at its peak emission wavelength of 530 nm. Optimal values for $\alpha=0.93$ and order L=3 were obtained, and two exponential terms were also used.
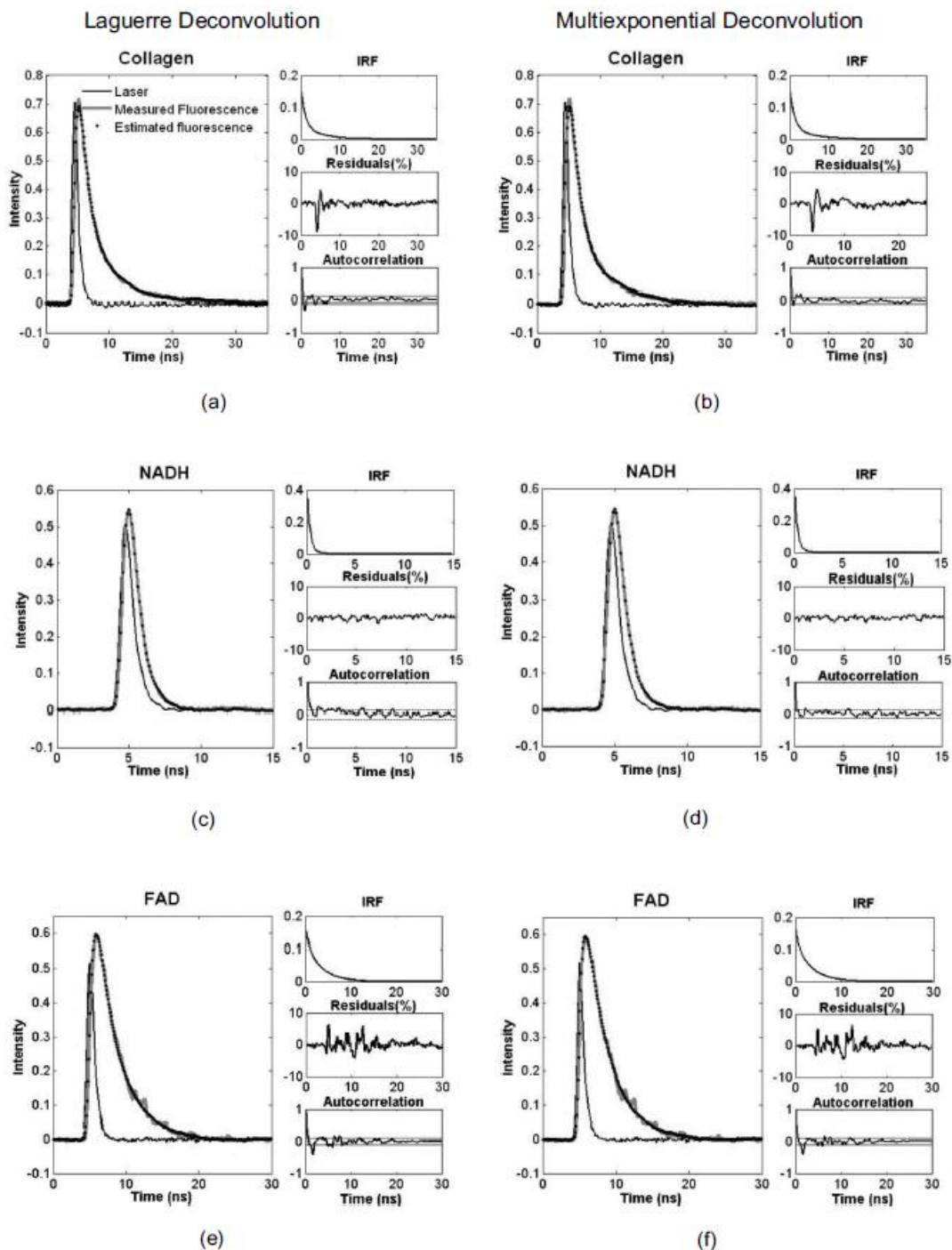
Figure 5. Deconvolution results of the TRFS data from the tissue constituents.
(a) and (b), collagen at 400nm, (c) and (d), NADH at 450 nm and (e) and (f) FAD at 530 nm using the Automated Laguerre (left and multiexponential (right) methods. The fluorescence IRFs were accurately estimated by both methods

Table 1. Estimated lifetime values from fluorescence standards and tissue constituents. Multiexponetial model (with LSIR) was implemented using two exponential terms in the expansion.

Sample	Solvent	Wave-length (nm)	Opt. α	Opt. order	Lifetime (ns)		
					Auto. Laguerre	LSIR	Literature
9-CA	Ethanol	450	0.96	4	12.61 ± 0.58	12.18 ± 0.73	11.7-12.28
Rhodamin B	Ethanol	580	0.84	4	2.52 ± 0.10	2.44 ± 0.14	2.60-3.01
Rhodamin B	H_2O	580	0.74	4	1.55 ± 0.03	1.58 ± 0.05	1.48-1.67
Rose Bengal	Ethanol	570	0.62	3	0.65 ± 0.02	0.61 ± 0.01	0.84
Rose Bengal	Methanol	570	0.57	3	0.48 ± 0.01	0.48 ± 0.01	0.54
Collagen	N/A	400	0.91	3	1.56 ± 0.07	1.65 ± 0.07	1.05-1.42
NADH	PBS	450	0.67	4	0.45 ± 0.03	0.36 ± 0.01	0.30-0.40
FAD	PBS	530	0.93	3	2.24 ± 0.12	2.29 ± 0.12	2.30-2.85

Table 2. Comparison of computation time using automated Laguerre and traditional methods. Multiexponential model was implemented using two exponential terms in the expansion.

Sample	Solvent	Computation Time (ms)		
		Laguerre	Auto. Laguerre	LSIR
9CA	Ethanol	7	266	153
Rhodamin B	Ethanol	5	258	67
Rhodamin B	H20	5	193	68
Rose Bengal	Ethanol	3	69	45
Rose Bengal	Methanol	3	32	73
Collagen	N/A	3	175	366
NADH	PBS	4	54	139
FAD	PBS	3	157	779

Table 2 compares the computational speed of the proposed method with the original Laguerre method (without optimization) and the LSIR method which uses the multi-exponential model. The automated Laguerre deconvolution method appears to be slower than the original Laguerre method. This result is expected because the automated Laguerre method performs a complete optimization of the alpha parameter using non-linear least squares, searches for the appropriate expansion order and also adjusts for the zero-time delay. However, it can be seen from Table 2 that the automated Laguerre has computation times quite comparable to the multiexponential method while providing with a more robust data analysis technique for TRFS.

To illustrate the sensitivity of the figure of merits used for optimizing orders and delays, Figure 6 shows the MDL value as a function of order and the NMSE value as a function of delay, corresponding to the FAD fluorescence decay deconvolution. The left panel shows how the MDL value decreases significantly from an order 2 to an order 3 estimation, but does not change significantly for orders higher than 3. Based on this, an optimal order L=3 was successfully found. In the right panel, it is shown how the NMSE reaches an absolute minimum at a delay of 0.8 ns, clearly showing that this is the time difference between the measured fluorescence pulse and instrument response. These results indicate that the MDL and NMSE values are adequate criteria for searching optimal expansion order and zero-time delay, respectively.
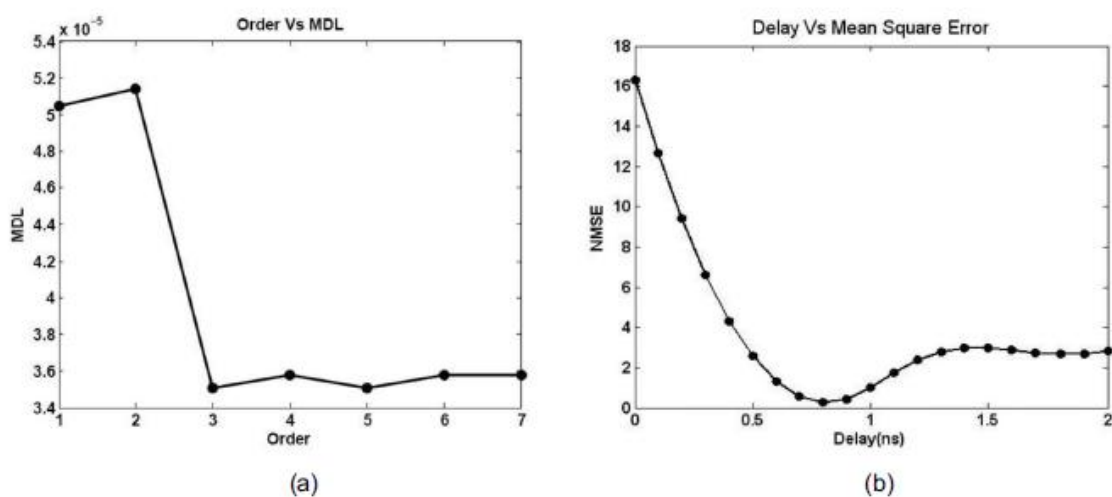
Figure 6. Values of MDL versus order (a) and NMSE versus zero-time delay (b) corresponding to the FAD fluorescence decay deconvolution

4.2 Validation on TRFS ex-vivo measurement from human arteries

Finally, the proposed automated Laguerre deconvolution method was also validated on TRFS data obtained from human arteries ex-vivo. Deconvolution results from sample artery fluorescence decay are shown in Figure 7. For this particular case, optimal values

for alpha=0.88 and order L=5 were obtained, and two exponential terms were used. Based on the low residuals level (<5%) and flat autocorrelation function, it can be observed that both the Laguerre and the multiexponential methods successfully deconvolved the artery TRFS data.
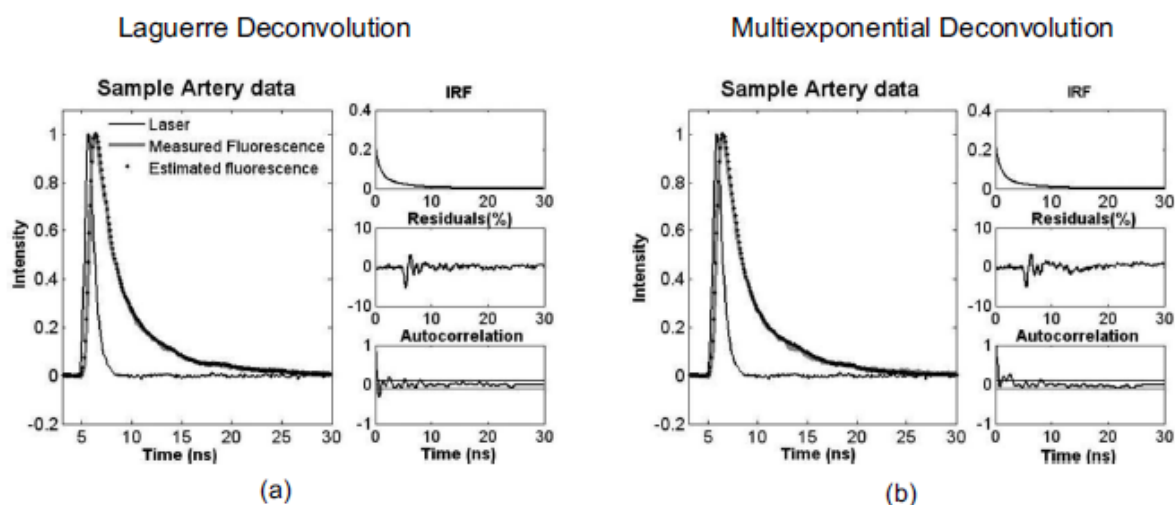

Figure 7. Deconvolution results from a sample of human artery TRFS data using the automated Laguerre deconvolution (a) and multiexponential (b) methods.

In addition, it was important to assess ranges of values the parameter α, the order L and the delay, that were optimal for deconvolving human arterial TRFS data. For this purpose, the average values of these parameters (mean ± SE) were estimated as a function of wavelengths from all data sets collected. Results of this analysis are shown in Figure 8. It was observed that the optimal α values for accurate deconvolution of arterial TRFS data were between 0.9-0.95, and there was no obvious variation in α values with emission wavelengths (Figure 8.a). The optimal orders were usually either 4 or 5, and there was no apparent correlation between them and the emission wavelengths (Figure 8.b). The zero-shift delay, on the other hand, was highly correlated with emission

wavelength, going from ~0.5 ns at 400 nm to ~0.95 ns at 550 nm, with an almost linear increase of delay with the emission wavelength (Figure 8.c). The average NMSE was estimated as a function of emission wavelength, which indicate excellent estimation performance for all wavelengths (NMSE < 2%) (Figure 8.d).
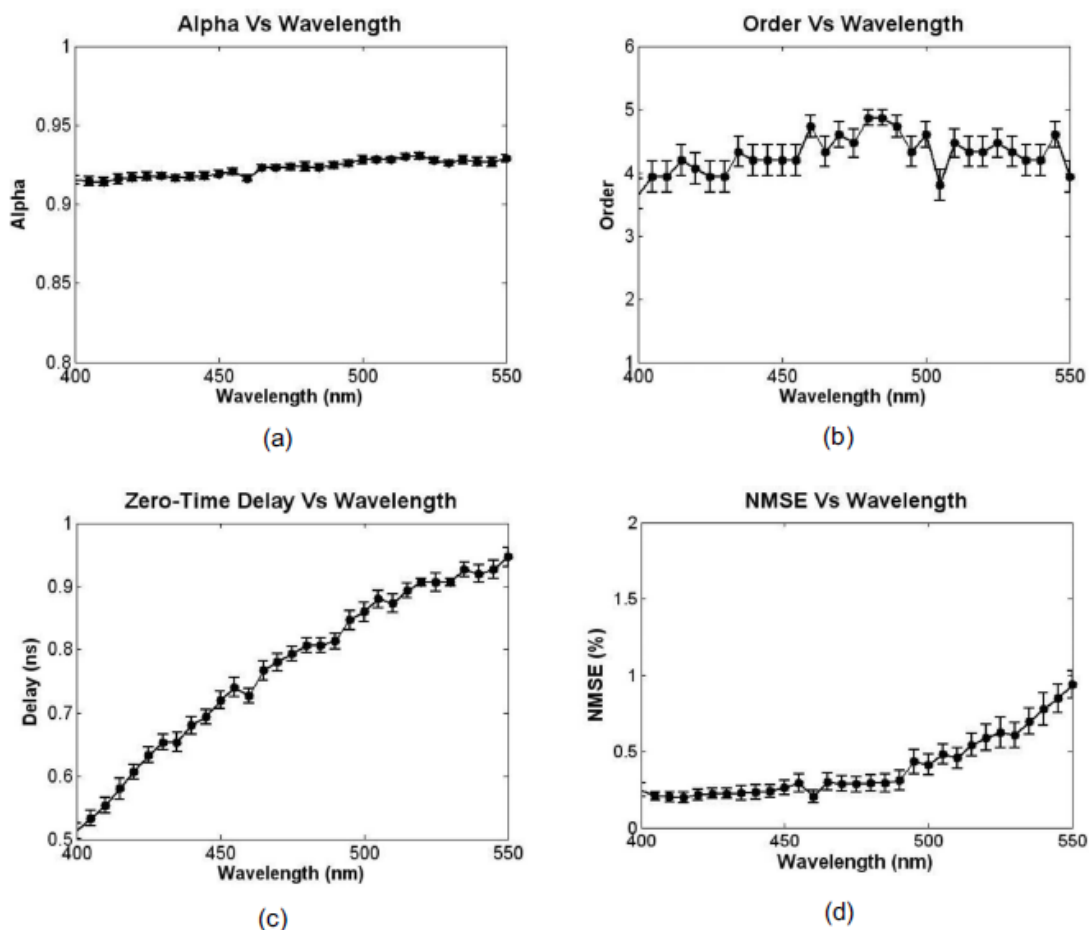

Figure 8. Statistics on results from artery samples.
Average (mean ± SE from 47 artery datasets) values for (a) the Laguerre parameter α, (b) expansion order, (c) zero time delay (d) NMSE as a function of emission wavelengths from all human artery TRFS datasets.

CHAPTER V

DISCUSSION, CONCLUSION AND FUTURE WORK

5.1 Discussion

In this thesis, a new fully automated deconvolution method for TRFS data analysis has been presented, based on an optimized iterative Laguerre expansion algorithm. The advantage of the Laguerre deconvolution method over the classical multiexponential least-square iterative reconvolution (LSIR) approach has been reported [26], especially for analyzing complex fluorescence systems, such as biological tissues. One big limitation, however, from this first version of the Laguerre deconvolution method, was the need to select a priori optimal values for the parameter α and the expansion order (model parameters) that would guarantee accurate estimation of the fluorescence IRF. To overcome this limitation, an iterative version of the Laguerre deconvolution method has been developed, in which no a priori assumption on these parameters is needed. In addition, the proposed method also takes into consideration the well known emission wavelength dependence of the zero-time shift or delay of the instrument response with respect to the fluorescence decay. The proposed method was successfully validated on fluorescence lifetime standards, fluorescence tissue constituents, and human tissue. The following is a discussion of the validation results and of the advantages of the proposed automated Laguerre deconvolution method.

The validation results on TRFS data from fluorescence lifetime standards and tissue components show that both the automated Laguerre deconvolution and the classical LSIR

methods were able to estimate the underlying fluorescence IRF and lifetime values, which were in well agreement with the literature (Table 1). One important advantage of the method was that the model parameters were automatically optimized, while for the case of the LSIR method, the number of exponentials needed for accurate deconvolution was found by trial and error. The other significant advantage of the proposed method was the ability to estimate the real zero-order delay between the instrument response and the measured fluorescence decay. As a matter of fact, the optima delay found using the automated Laguerre approach was also applied before performing the LSIR method, so the last one could converge correctly to an optimal estimation of the fluorescence IRF.

Another important observation was the correlation between the optimal parameter α obtained by the proposed method and the underlying fluorescence lifetime of the estimated IRF. From Table 1 it can be observed that long lived fluorescence IRF (e.g. 9CA) are better expanded using large α values, while short lived IRF (e.g. rose Bengal) are usually well estimated with smaller α values. This is consistent with previous results obtained using the original Laguerre deconvolution implementation. In the original Laguerre deconvolution implementation, however, the value of α is user selected by trial and error until adequate expansion of the fluorescence IRF is attained. In contrast, in the current version, optimal values for α are automatically estimated from the data by using a nonlinear least square approach. This represents a significant advantage over the previous method, since it will allow using the Laguerre deconvolution method in numerous applications where online analysis of TRFS data is required. With regard to the introduction of TRFS to clinical applications, the automated Laguerre deconvolution

algorithm need to be incorporated into the existing TRFS instrumentation, in order to achieve real-time acquisition and analysis of TRFS data.

Model complexity quantification is a very well studied problem in the field of mathematical modeling and system identification [34]. A number of model complexity figures have been proposed, aiming to determine the level of complexity needed by a given model to properly account for the dynamics being investigated. Among the numerous complexity figures being proposed, the MDL is one of the most robust and widespread used[33-34]. The Laguerre deconvolution method constitutes a modeling problem, in which the fluorescence IRF is modeled as a linear expansion of Laguerre functions. At such, the model complexity is directly linked to the expansion order L. The proposed results clearly demonstrated that the MDL can be successfully used for quantifying the expansion complexity, therefore, determining the optimal expansion order needed for accurate fluorescence IRF expansion. As shown in Figure 4.a as an example, the MDL value usually decreases as the order expansion increases, until an optimal order is reached, after which the MDL values does not further decreases significantly. Since the MDL criterion sacrifice model estimation for level of complexity, in some instances it is convenient to choose a higher order than the one determined by MDL in order to warranty good fluorescence IRF estimation. Such heuristic rules can be easily implemented on the proposed algorithm.

During TRFS measurement, the instrument response cannot always be acquired at the same emission wavelength as the recorded fluorescence decay [40-41]. Since the

refractive index of the various optical materials present in a TRFS instrument depend on the photon wavelengths, the instrument response and fluorescence pulses may travel at different speed throughout the TRFS instrumentation. Because of this speed difference, the instrument response and the measured fluorescence pulse may arrive with a relative time delay between each other. Thus, during the deconvolution process, it may be necessary to account for this zero-time shift or delay. Making the assumption that the optimal fluorescence IRF estimation is achieved when both the instrument response and fluorescence pulse are aligned in time (zero delay), we decided to use a goodness of the fit index, such as the NMSE, to estimate the experimental zero-time delay. As shown in Figure 6.b as an example, the NMSE usually show a global minimum at the optimal delay, allowing a systematic determination of the zero-time shift.

For the past several years, TRFS have been evaluated as a potential clinical tool for minimally invasive and nondestructive tissue diagnosis. A few groups have shown the potential of TRFS for detecting difference in tissue biochemical composition related to pathological conditions [1-3, 5-6, 36, 42]. As a progression of this particular study, the next area of focus would be on validating time-resolved fluorescence measurements (spectroscopy and imaging) for characterizing the biochemical composition of atherosclerotic plaques, which is clinically relevant for detecting those patients with high risk of heart attacks and stroke. This made it essential to further validate method on TRFS data obtained from human arteries in-vivo. The results (Figure 5 and 6.d) clearly indicate a very good performance by the proposed automated Laguerre deconvolution method for

estimating human artery fluorescence IRF and lifetimes throughout the whole emission spectrum.

In addition, it will also be valuable to investigate what values of the parameter α were optimal for accurate deconvolution of human artery TRFS data. The proposed results (Fig. 6.a) showed that optimal values for α were concentrated within a range of 0.8-0.9 with no apparent correlation between α and the emission wavelength. These findings indicate that it may be possible to speed up the optimization of the parameter α, for instance, by assigning an initial condition within the interval 0.8-0.9 for the nonlinear least-square algorithm. In the extreme case, it may be even feasible to use a fixed valued for α (e.g. α = 0.85) that would be close to optimal for deconvolving any arterial TRFS. This hypothesis will be tested as part of the proposed future research.

Similarly, it was also investigated how many Laguerre functions were necessary for accurate estimation of arteries fluorescence IRF. The results (Fig. 6.b) showed that optimal expansion orders were usually either 4 or 5, regardless of the emission wavelength. These findings suggest that we can limit the search for the optimal order in a much reduced interval (e.g. 3-5), which would significantly increase the computational speed of the method. As in the case of the parameter α, in the extreme case, it may be even suitable to fix the expansion order to an upper bound of the optimal value (e.g. L=5) to ensure the goodness of the fit by slightly sacrificing model complexity. Again, this hypothesis will be tested as part of the future research.

As previously discussed, due to the wavelength-dependent refractive index of the optical materials travelled by light pulses in the TRFS instruments, it is not uncommon to observe a zero-time delay between the recorded instrument response and measured fluorescence pulses. In the particular TRFS instrument, both the scattering light of the excitation laser (instrument response) and the sample fluorescence emission are collected through a silica/silica step index optical fiber bundle. Since the refractive index of this fiber is higher for shorter than for longer wavelengths, fluorescence pulses at longer wavelengths than the excitation wavelength travel faster than the measured scattered instrument response. Thus, the instrument response is usually delayed with respect to the fluorescence pulse, and the delay is expected to increase at longer fluorescence emission wavelengths. The results from arteries are in agreement with this phenomenon, as it can be observed how the delay of the instrument response with respect to the fluorescence pulse increases with the emission wavelength (Figure 6.c). These results underscore the need for taking into consideration the zero-time delay for proper estimation of the fluorescence IRF, especially for TRFS instruments with high temporal resolution.

The validation results on the human artery TRFS data are of special relevance for the research on TRFS based diagnosis of atherosclerosis. The findings discussed above suggest the possibility of customizing the proposed automated Laguerre deconvolution method for online analysis of arterial TRFS data. For instance, a TRFS instrument could be characterized and calibrated, in order to determine suboptimal values for zero-time delay at specific wavelength, and let the algorithm search around these for the optimal delay values. In addition and as discussed before, a fixed expansion order could be

predefined as well. Finally, since optimal α values for deconvolving arterial TRFS are limited to a narrow range (0.8-0.9), a customized and faster version of the algorithm can be implemented to search only in that relevant interval. Similar approaches for customizing the automated Laguerre deconvolution method for a specific type of samples (e.g. a given tissue of interest) will be also useful for facilitating online application of TRFS in numerous other areas (e.g. chemistry, biochemistry, drug development).

Perhaps, the only drawback of the current version of the automated Laguerre deconvolution method is its slower performance with respect to the original implementation[26]. This is understandable, since a full model parameter optimization is performed in the automated version, the parameter α is optimized by nonlinear least-square minimization, and both the order and delay values are optimized by exhaustive searching of values minimizing a complexity (MDL) and performance (NMSE) figures of merit, respectively. On the other hand, no user intervention is required for tuning up the model parameters, allowing online analysis of TRFS data. Furthermore, and as discussed above, the method can be customized for a given sample type and TRFS instrumentation in order to speed up its performance.

5.2 Future scope

The future possibilities for this study include extending the automated Laguerre deconvolution method for fluorescence lifetime imaging microscopy (FLIM) data analysis. In the context of FLIM, the analysis of a single image requires deconvolution of the instrument response from the fluorescence decay of each pixel within the field of

view. A Laguerre expansion based approach for FLIM data deconvolution has been demonstrated that performs at least two orders of magnitude faster than standard FLIM deconvolution algorithms [43]. As for the case the case of original Laguerre TRFS deconvolution, the current Laguerre FLIM deconvolution also requires to select the expansion parameters (i.e. α and order) by trial and error. Thus, an automated version of the Laguerre FLIM deconvolution method would facilitate the use of this novel technique in various applications, including ongoing research on FLIM based atherosclerosis and cancer diagnosis.

5.3 Conclusion

In summary, a new fully automated deconvolution method for TRFS data analysis based on an iterative Laguerre expansion approach has been presented. The method has been extensively validated on TRFS data from fluorescence lifetime standards, tissue constituents and human tissue ex-vivo. The main advantage of the method is that it does not require any user intervention for tuning up the deconvolution process. The method is expected to facilitate the use of TRFS in applications where online data analysis is required.

REFERENCES

[1]   J. A. Jo, Q. Fang, T. Papaioannou ,J. H. Qiao, M.C. Fishbein, et al., "Diagnosis of vulnerable atherosclerotic plaques by time-resolved fluorescence spectroscopy and ultrasound imaging," *28th Annual International Conference of the IEEE Engineering in Medicine and Biology Society*, vol. 1, pp. 2663-266, August 2006 .

[2]   L. Marcu, Q. Y. Fang, J. A. Jo, T. Papaioannou, A. Dorafshar, et al., "In vivo detection of macrophages in a rabbit atherosclerotic model by time-resolved laser-induced fluorescence spectroscopy," *Atherosclerosis*, vol. 181, pp. 295-303, Aug 2005.

[3]   L. Marcu., M. C. Fishbein, J. M. Maarek, W. S. Grundfest, "Discrimination of human coronary artery atherosclerotic lipid-rich lesions by time-resolved laser-induced fluorescence spectroscopy," *Arterioscler. Thromb. Vasc. Biol*, vol. 21, pp. 1244-1250, Jul 2001.

[4]   L. Marcu, J. A. Jo, P. V. Butte, W. H. Yong, B. K. Pikul, et al., "Fluorescence lifetime spectroscopy of glioblastoma multiforme," *Photochem. Photobiol.*, vol. 80, pp. 98-103, Jul.-Aug. 2004.

[5]   M. A. Mycek, K. T. Schomacker, N. S. Nishioka, "Colonic polyp differentiation using time-resolved autofluorescence spectroscopy," *Gastrointest. Endosc.*, vol. 48, pp. 390-4, Oct 1998.

[6]   T. J. Pfefer, D. Y. Paithankar, J. M. Ponero, K. T. Schomacker, N. S. Nishioka, "Temporally and spectrally resolved fluorescence spectroscopy for the detection of high grade dysplasia in Barrett's esophagus," *Lasers in Surgery and Medicine*, vol. 32, pp. 10-16, 2003.

[7]   J. R. Lakowicz, *Principles of Fluorescence Spectroscopy*, 3rd ed., Springer, 2006.

[8]   W. M. Vaughn and G. Weber, "Oxygen quenching of pyrenebutyric acid fluorescence in water. Dynamic probe of the microenvironment," *Biochemistry*, vol. 9, pp. 464-473, 2002.

[9]   J. Lippincott-Schwartz, E. Snapp, A. Kenworthy., "Studying protein dynamics in living cells," *Nat. Rev. Mol. Cell. Biol.*, vol. 2, pp. 444-456, 2001.

[10]   F. Stracke, C. Blum, S. Becker, K. Mullen, A. Meixner, "Correlation of Emission Intensity and Spectral Diffusion in Room Temperature Single-Molecule Spectroscopy," *Chem. Phys. Chem.*, vol. 6, pp. 1242-1246, 2005.

[11]   S. Andersson-Engels, J. Johannson, K. Svanberg, S. Svanberg, "Fluorescence imaging and point measurements of tissue, applications to the demarcation of

malignant tumors and atherosclerotic lesions from normal tissue," *Photochem. Photobiol.*, vol. 53, pp. 807-14, Jun 1991.

[12]   J. M. I. Maarek, L. Marcu, W. J. Snyder, W. S. Grundfest , "Time-resolved fluorescence spectra of arterial fluorescent compounds, Reconstruction with the Laguerre expansion technique," *Photochemistry and Photobiology*, vol. 71, pp. 178-187, Feb 2000.

[13]   L. Marcu, W. S. Grundfest J. M. I. Maarek, "Photobleaching of Arterial Fluorescent Compounds, Characterization of Elastin, Collagen and Cholesterol Time-resolved Spectra during Prolonged Ultraviolet Irradiation," *Photochemistry and Photobiology*, vol. 69, pp. 713-721, 1999.

[14]   C. Deka, B. E. Lehnert, N. M. Lehnert, G. M. Jones, L. A. Sklar, et al., "Analysis of fluorescence lifetime and quenching of FITC-conjugated antibodies on cells by phase-sensitive flow cytometry," *Cytometry*, vol. 25, pp. 271-279, 1996.

[15]   Y. Wu, Z Wei, J. Y. Qu, "Sensing cell metabolism by time-resolved autofluorescence," *Opt. Lett.*, vol. 31, pp. 3122-3124, 2006.

[16]   P. V. Butte, B. K. Pikul, A. Hever, W. H. Yong, K. L. Black, et al., "Diagnosis of meningioma by time-resolved fluorescence spectroscopy," *J. Biome.d. Opt.*, vol. 10, p. 064026, Nov-Dec 2005.

[17]   W. R. Ware, L. J. Doemeny, T. L. Nemzek, "Deconvolution of Fluorescence and Phosphorescence Decay Curves - Least-Squares Method," *Journal of Physical Chemistry*, vol. 77, pp. 2038-2048, 1973.

[18]   A. Grinvald and I. Z. Steinberg, "On the analysis of fluorescence decay kinetics by the method of least-squares," *Analytical Biochemistry*, vol. 59, pp. 583-598, 1974.

[19]   K. C. Lee, J. Siegel, S. E. Webb, S. Leveque-Fort, M. J. Cole, et al, "Application of the stretched exponential function to fluorescence lifetime imaging," *Biophys. J.*, vol. 81, pp. 1265-74, Sep 2001.

[20]   V. Marmarelis, "Identification of nonlinear biological systems using laguerre expansions of kernels," *Annals of Biomedical Engineering*, vol. 21, pp. 573-589, 1993.

[21]   J. Jo, A. Blasi, E. Valladares, R. Juarez, A. Nahdur, M. Khoo, "A Nonlinear Model of Cardiac Autonomic Control in Obstructive Sleep Apnea Syndrome," *Annals of Biomedical Engineering*, vol. 35, pp. 1425-1443, 2007.

[22] G. D. Mitsis and V. Z. Marmarelis, "Modeling of Nonlinear Physiological Systems with Fast and Slow Dynamics. I. Methodology," *Annals of Biomedical Engineering*, vol. 30, pp. 272-281, 2002.

[23] J. A. Jo, Q. Fang, T Pappaioannou, J. D. Baker, A. H. Dorafshar, et al., "Laguerre-based method for analysis of time-resolved fluorescence data, application to in-vivo characterization and diagnosis of atherosclerotic lesions," *J. Biomed. Opt.*, vol. 11, p. 021004, Mar-Apr 2006.

[24] J. A. Jo, Q. Fang, T Pappaioannou, M. C. Fishbein, B Besseth, et al., "Application of the Laguerre Deconvolution Method for Time-Resolved Fluorescence Spectroscopy to the Characterization of Atherosclerotic Plaques," *Engineering in Medicine and Biology Society, 2005. IEEE-EMBS 2005. 27th Annual International Conference of the*, pp. 6559-6562, Sept. 2005 2005.

[25] W. H. Yong, P. V. Butte, B. K. Pikul, J. A. Jo, Q. Fang, et al., "Distinction of brain tissue, low grade and high grade glioma with time-resolved fluorescence spectroscopy," *Front. Biosci.*, vol. 11, pp. 1255-63, 2006.

[26] J. A. Jo, Q. Fang, T Pappaioannou, L. Marcu, et al., "Fast model-free deconvolution of fluorescence decay for analysis of biological systems," *Journal of Biomedical Optics*, vol. 9, pp. 743-752, Jul-Aug 2004.

[27] S. Weiss, "Fluorescence Spectroscopy of Single Biomolecules," *Science*, vol. 283, pp. 1676-1683, March 12, 1999 1999.

[28] J. R. Lakowicz, A. Balter, "Analysis of fluorescence decay kinetics from variable-frequency phase shift and modulation data," *Biophys. J.,* vol. 46, pp. 463-77, Oct 1984.

[29] W. Becker, H. Hickl, C. Zander, K. H. Drexhage, M. Sauer, et al., "Time-resolved detection and identification of single analyte molecules in microcapillaries by time-correlated single-photon counting (TCSPC)," *Review of Scientific Instruments,* vol. 70, pp. 1835-1841, 1999.

[30] A. C. Mitchell, J. E. Wall, J. G. Murray, C. G. Morgan, "Direct modulation of the effective sensitivity of a CCD detector, a new approach to time-resolved fluorescence imaging," *Journal of Microscopy*, vol. 206, pp. 225-232, 2002.

[31] C. A. Buhler, U. Graf, A. R. Hochstrasser, M. Anliker, "Multidimensional fluorescence spectroscopy using a streak camera based pulse fluorometer," *Review of Scientific Instruments*, vol. 69, pp. 1512-1518, 1998.

[32] Q. Y. Fang, T. Pappaioannou, J. A. Jo, R. Vaitha, K. Shastry, et al., "Time-domain laser-induced fluorescence spectroscopy apparatus for clinical diagnostics," *Review of Scientific Instruments*, vol. 75, pp. 151-162, Jan 2004.

[33]   P. Grünwald, "Model Selection Based on Minimum Description Length," *Journal of Mathematical Psychology,* vol. 44, pp. 133-152, 2000.

[34]   L. Ljung, *System identification, Theory for the user*, 2nd ed. Upper Saddle River, NJ, Prentice Hall PTR, 1999.

[35]   F. De Ridder, R. Pintleton, J. Schoukens, D. P. Gillikin, "Modified AIC and MDL model selection criteria for short data records," *Instrumentation and Measurement, IEEE Transactions on*, vol. 54, pp. 144-150, 2005.

[36]   N. Ramanujam, "Fluorescence spectroscopy of neoplastic and non-neoplastic tissues," *Neoplasia,* vol. 2, pp. 89-117, Jan-Apr 2000.

[37]   R. Richards-Kortum and E. Sevick-Muraca, "Quantitative optical spectroscopy for tissue diagnosis," *Annu Rev Phys Chem,* vol. 47, pp. 555-606, 1996.

[38]   N. Boens,W. Qin, N. Basari, J. Hofken, M. Ameloot, et al, "Fluorescence lifetime standards for time and frequency domain fluorescence spectroscopy," *Anal Chem,* vol. 79, pp. 2137-49, Mar 1 2007.

[39]   D. P. Jonathan and M. Mary-Ann, "Design and development of a rapid acquisition laser-based fluorometer with simultaneous spectral and temporal resolution," *Review of Scientific Instruments*, vol. 72, pp. 3061-3072, 2001.

[40]   M. Van Den Zegel, N. Boens, D. Daems, F. C. DeSchryver, "Possibilities and limitations of the time-correlated single photon counting technique, a comparative study of correction methods for the wavelength dependence of the instrument response function," *Chemical Physics,* vol. 101, pp. 311-335, 1986.

[41]   R. Luchowski, Z. Gryczynski, P. Sarkar, J. Borejdo, M. Szableski, et al., "Instrument response standard in time-resolved fluorescence," *Review of Scientific Instruments*, vol. 80, pp. 033109-6, 2009.

[42]   L. Marcu, J. A. Jo, Q. Y. Fang, T. Pappaioannou, J. H. Qiao, et al., "Detection of high-risk atherosclerotic plaques by time-resolved laser induced fluorescence spectroscopy," *Circulation,* vol. 112, pp. U678-U678, Oct 25 2005.

[43]   J. A. Jo, Q. Fang, L. Marcu, "Ultrafast method for the analysis of fluorescence lifetime imaging microscopy data based on the Laguerre expansion technique," *Selected Topics in Quantum Electronics, IEEE Journal of*, vol. 11, pp. 835-845, July-Aug. 2005 2005.

[44]   University of California, Berkeley, The IceCube research group, http://icecube.berkeley.edu/~bramall/work/astrobiology/fluorescence.htm

[45] Molecular expressions - Microscopy primer,
http://www.microscopy.fsu.edu/primer/techniques/fluorescence/fret/fretintro.html

VITA

Name,   Aditi Sandeep Dabir

Address,   Department of Biomedical Engineering,
                 337, Zachry Engineering Center
                 3120, TAMU
                 Texas A&M University
                 College Station, TX 77843-3120

Email Address,   aditidabir@gmail.com

Education,   M.S. Biomedical Engineering, Texas A&M University
                 B.E. Instrumentation and Control, University of Pune, India